Journal of Thermal Analysis and Calorimetry, Vol. 81 (2005) 197–203

THERMAL ANALYSIS AT THE EVALUATION OF CONCRETE DAMAGE BY HIGH TEMPERATURES

I. Janotka[1*] *and S. C. Mojumdar*[2]

[1]Institute of Construction and Architecture, Slovak Academy of Sciences, Dúbravská 9, 845 03 Bratislava 45, Slovakia
[2]Institute for Research in Construction, National Research Council, Government of Canada, M-20, 1200 Montreal Road, Ottawa, Ontario, K1A 0R6, Canada

Concrete damage by high temperatures includes mass loss, strength and modulus reductions and the formation of cracks and large pores. Thermal treatment reduces the amount of chemically bound water in the hydrate phase. With a rise in temperature, the spatial distribution of $Ca(OH)_2$ crystals becomes more compact; smaller crystals occur in a unit volume of the cement paste. A rise in temperature affects the pore structure by reducing the specific surface of hydration products. Cement paste becomes more heterogeneous in microstructure and coarser in pore structure. Compressive strength is not only significant parameter showing structural integrity of concrete; permeability influences concrete durability as well. To demonstrate this, permeability coefficients at various high temperatures are presented. The key quantitative insight into the hydrate phase behavior is based on thermal analysis results. Thermogravimetric (TG) mass losses are related to the phase changes represented either by DTA or DTG. Based on these, the tests employing TG mass losses and related DTA and DTG curves answer the question if the hydrate phase is present at individual high-temperature levels and what its quantitative state is. Method of thermal analysis is suitable for the interpretation of concrete behavior when subjected to high-temperature attack.

Conclusions are drawn about thermal stability and residual properties of concrete specimens made at the construction site of Mochovce nuclear power plant (Slovakia); and subjected to temperatures up to 800°C. Relations among mechanical properties, permeability, pore median radius and bound water content in concrete are discussed and evaluated.

Keywords: *cement paste, concrete high temperature, permeability, porosity, thermal analysis*

Introduction

Concrete is recognized as an excellent thermal-resistant building material. With the use of concrete in certain building constructions, additional information is required on the effect of high-temperature attack on concrete. Much has been learned about mechanical and engineering properties in situations of high-temperature exposure [1–6]. Next important factors that influence the behavior of concrete at high temperatures are the heating rate [7], the type of binder and aggregate [8–11] and the moisture conditions [12–14]. Direct dependence between pore size values and calculated permeability coefficients were found. Concrete damage at temperature elevations is shown by an average pore radius increase. The bulk density of cement paste in concrete; mainly between 400 and 800°C decreases with rise in total porosity. Density in the same temperature range increases due to higher density of new compounds formed after the cement paste thermal decomposition, and more pores are included in concrete samples with coarser pore structure [15].

The loss in mechanical properties and the increase in total porosity of concrete are influenced by its degradation through changes induced in basic processes of cement hydration and hardening of the bonding system in the cement paste under the high-temperature attack. The sensitivity of C–S–H gel to achieved temperature level is evident from average C–S–H composition at 25°C $C_{1.88}SH_{1.52}$ and at 100°C $C_{2.04}SH_{0.98}$ [14]. These results clearly show the influence of temperature on the C/S and H/S ratios of C–S–H gel. Thermal treatment reduces the amount of bound water and increases the calcium content of C–S–H gel [16,17]. The high temperature tends to change the mechanism of ettringite formation; a marked reduction in stability of ettringite between 60 and 80°C is observed. Ettringite hydrates begin to dehydrate within this temperature range and ettringite ruptures and disintegrates [18]. Moreover, it seems that the decomposition of ettringite lowers the OH^- concentration of the pore water solution [19]. The $Ca(OH)_2$ crystals are sheet-like and have an elongated shape at ambient temperature [20, 21]. With a rise in temperature, the spatial distribution of $Ca(OH)_2$ crystals becomes more compact. It means smaller crystals occurring in a unit volume of the cement paste [22]. This is connected by decreased solu-

* Author for correspondence: ivan.janotka@savba.sk

1388–6150/$20.00

Akadémiai Kiadó, Budapest, Hungary
Springer, Dordrecht, The Netherlands

bility of $Ca(OH)_2$ at higher temperatures. By contrast, hydrated cement pastes at lower temperature are more likely to contain large masses of $Ca(OH)_2$, with a well-developed morphology [23]. A rise in temperature affects the cement paste pore structure by reducing the specific surface of hydration products. Cement paste exposed to high-temperature attack is more heterogeneous in a microstructure and coarser in pore structure [24, 25]. The decrease in volume of the hydrate phase and $Ca(OH)_2$, and the coarsening of the pore structure of concrete are the main reasons influencing engineering properties decrease at high-temperature attack.

The present paper is concerned with thermal stability and residual properties of concrete specimens from a construction site of Mochovce nuclear power plant (Slovakia), subjected to temperatures up to 800°C. Relations among mechanical properties, permeability, pore median radius and bound water content of the cement paste and concrete are discussed and evaluated as well.

Experimental

Materials

Blastfurace slag Portland cement (CEM II / B-S 32.5 R) and siliceous river gravel were chosen for the investigation. The composition and properties of the fresh concrete are listed in Table 1.

Table 1 Composition and basic properties of concrete mixture

Components	Content per 1 m^3
Cement II/B-S 32.5 R	485.0 kg
Aggregates 0–4 mm, river gravel	880.0 kg
Aggregates 8–16 mm, river gravel	880.0 kg
Drink water	170.0 L
Water to cement ratio, W/C	0.35
The portion of smectite in aggregate smaller than 0–4 mm	1.6%
The moisture content in aggregate	3.9%
Fresh concrete	
Temperature	16.7ºC
Volumetric density	2 356.0 kg m^{-3}
Workability: Abrams	75.0 mm
Ve–Be	1.5 s
Air content (no air entraining agent used)	1.8 % vol.

Casting

The fresh concrete used to make prisms (100x100x400 mm) was made in steel moulds on a vibration table (50 Hz, 0.35 mm) with vibration time of 30 s. The workability tests of fresh concrete according to STN ISO 4109 (the slump by Abrams equipment, equivalent to ASTM C 143) and STN ISO 4110 (the flow by Ve-Be time consistometer, equivalent to BS 1881-prEN 12350) were performed after mixing.

Curing and heating

Following removal from the moulds, all specimens were stored at 20°C and 100% relative humidity (RH) wet air for 28 days. Heating regime 1 (HR1) concerns the increase of temperature to 40, 60, 100 and 200°C, whereas the temperature was increased to 60, 200, 400 and 800°C in heating regime 2 (HR2). Graphs of both applied heating regimes are shown in Figs 1 and 2, respectively.

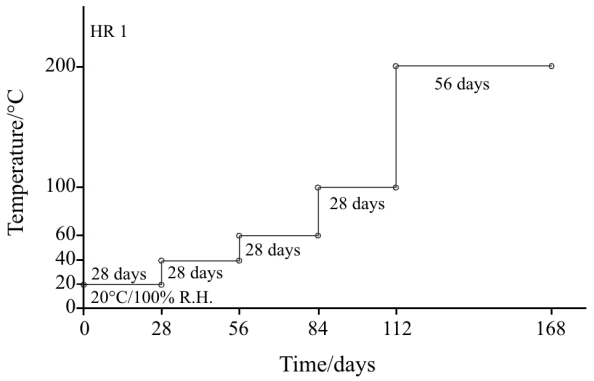

Fig. 1 Heating regime (HR 1) for concrete specimens attacked up to 200°C

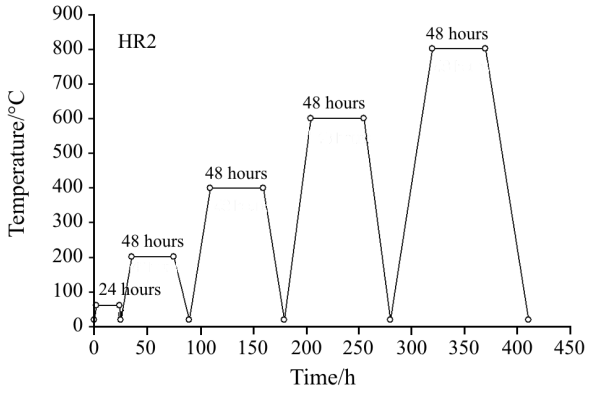

Fig. 2 Heating regime (HR 2) for concrete specimens exposed to temperatures up to 800°C

Testing

Physical-mechanical properties of the reference specimens cured for 28 days in wet air as well as those exposed to high temperatures were obtained. After the thermal exposure, the specimens were left to cool to the ambient 20°C prior to the next tests. Prismatic

specimens were tested to determine the dynamic and Young´s modulus of elasticity and their strengths.

The values of dynamic modulus of elasticity (DME) were calculated from

$$E_{bu} = \rho v_L^2 \frac{1}{k^2} 10^{-6} \quad (1)$$

where E_{bu} is the DME (GPa), ρ is the density of the prisms (kg m^{-3}), v_L^2 is the impulse speed of longitudinal ultrasonic waves (m s^{-1}) and k=1.0541 at Poisson coefficient ν_{bu}=0.20.

Young's modulus of elasticity was calculated according to STN ISO 6784 from

$$E_b = \frac{\Delta\sigma}{\Delta\varepsilon} = \frac{\sigma_a - \sigma_b}{\varepsilon_a - \varepsilon_b} \quad (2)$$

where σ_a is the stress on the stress level γ_σ =1/3 (MPa) (σ_a=f_c/3), where f_c is the compressive strength of concrete (MPa), σ_b is the starting stress (0.5 MPa), ε_a is average relative strain at the stress level ν_σ=1/3 (‰) and ε_b is the average relative strain at the starting stress (‰). The relation of per mille (‰) to micro strain (μs) is 1 μs=0.001‰.

The concrete pore structure was studied by mercury intrusion porosimetry (MIP) using the high-pressure porosimeter mod. 2000 and macroporosimeter mod. 120 (Carbo Erba Science, Milan). From the measured data, permeability coefficients of the concrete were calculated. Powder X-ray diffraction patterns were recorded on a Philips X-ray diffractometer coupled with an automatic data recording system. CuK_α radiation and Ni-filter were used. The thermal curves were recorded on a Derivatograph Q 1500 (MOM Budapest). In general, 200 mg of the sample was heated at 20 K min^{-1} from 20 to 1000°C.

Results and discussion

The compressive strength at 200°C in both heating regimes is higher than at 20°C. The assessment of concrete damage by temperatures between 20 and 200°C only by compressive strength values may give ambiguous results. The evident drop in strength of the specimens is observed at temperatures between 200 and 800°C (Fig. 6). Elasticity module evidently drop after 40°C; and decrease significantly after temperature exposures at 100°C (HR1) and 200°C (HR2), respectively (Table 2). It is believed that the main reason of such concrete behaviour is the quick release of moisture at lower temperatures (20–100°C) and bound water from hydrated minerals of the cement after a sudden rise in temperature between 100 and 800°C. At higher temperatures, an increase of the strain at the maximum stress appears in concrete specimens relative to those exposed only to lower temperatures. This may be the reason for the high sensitivity of Young's modulus of elasticity to the temperature attack. High temperatures contribute to the formation of large pore structures and result in the reduction of compressive strength and Young's modulus of elasticity. The decrease in volume of the hydration products and $Ca(OH)_2$, and the coarsening of pore structure of concrete are the main reasons influencing utility properties decrease at temperatures up to 800°C. The drop in strength and Young's modulus of elasticity, is the consequence of the concrete degradation through changes induced in basic processes of cement hydration on the achieved temperature level.

Table 2 Dynamic (E_{bu}) and Young's (E_b) module of elasticity of tested specimens subjected to HR1 heating regime

Curing regime	E_{bu} /GPa	E_b /GPa
20°C, 28 days (basic[a])	43.1	27.8
40°C + 28 days	40.1	29.7
60°C + 28 days	38.3	28.8
100°C + 28 days	34.1	27.7
200°C + 56 days	24.8	18.0
20°C/60% R.H.[b]	42.9	30.9

[a]28-day basic curing at 20°C and 100% R. H. – moist air, [b]Basic curing +140 days at 20°C and 60% R.H. – dry air

Pore structure characteristics and calculated permeability coefficients of the specimens are given in Table 3. The results reveal direct dependence between average micropore median radius, total pore median radius, total porosity, specific surface area and calculated permeability coefficients. Longer duration of temperature elevation at 200°C at heating regime 1 (28 days) relative to 2-day exposure at heating regime 2 gives coarser pore structure of the specimens. The explanation is to be found in differences of the pore structure development of concrete specimens cured at 200°C for different periods. It is believed that various types of hydration products in the cement paste form pore structures with diverse and markedly characteristics of pore size distribution. Pore structure depends either on the volume, type and properties of hydration products occurring in the cement paste; either on time of the high-temperature attack. The reasons for this fact are differences in the crystalline structure, morphology size and bound water content of individual particles of distinct types of hydration products at 200°C, and any other temperature elevation. The higher the temperature, the coarser the pore structure and the higher permeability concrete become. These changes, however, appear more expressly when the temperature is over 400°C. Permeabilities are valuable for assessing the struc-

Table 3 Mercury porosimetry measurements and calculated permeability coefficient for concrete specimens heated to 800°C

Curing	V_{MP}	V_{TP}	M_{MP}	M_{TP}	*MK*	*TP*	*SpS*	*F*	*K*
20°C	59.52	62.75	30.90	33.18	5.15	13.13	6.039	16	0.87
40°C	56.74	60.04	43.59	47.02	5.50	12.75	4.752	21	1.81
60°C	63.74	66.15	53.18	55.10	3.64	13.98	3.423	20	2.52
100°C	72.66	76.31	55.41	58.26	4.77	15.65	3.597	23	3.60
200°C	70.28	73.04	61.69	65.00	3.78	15.23	3.457	33	6.36
200°C	58.74	61.43	57.29	60.79	4.38	13.14	4.511	29	4.05
400°C	58.12	60.47	77.64	87.26	3.89	13.08	3.900	45	10.37
600°C	89.39	96.45	176.72	222.69	7.31	19.67	2.555	60	67.46
800°C	161.71	197.68	155.49	294.62	18.20	34.50	3.136	55	89.30

*HR*1=temperatures 20–200°C , HR2= temperatures 200–800°C V_{MP}, V_{TP}=volume of micropores (up to 7500 nm) and volume of all pores /$mm^3.g^{-1}$ M_{MP}, M_{TP} =average micropore median radius and total pore median radius /nm *MK*=portion of macropores /% *TP*=total porosity /% vol. *SpS*=pore specific surface /$m^2\ g^{-1}$ *F*=portion of pores in the radius range of 100-10000 nm /% *K*=permeability coefficient /*10^{-10} $m.s^{-1}$

tural integrity of concrete subjected to high temperatures, and appear as good and useful as the measured Young's module of elasticity and compressive strengths.

The above data undoubtedly confirm the phenomenon of pore structure coarsening due to temperature elevation. It is evident from the comparison of porosity data. The explanation is that the bulky material of the products of cement hydration is replaced by air voids. This exhibits a marked concrete strength decrease mainly over 400°C. The temperature 800°C characterizes the collapse of the concrete's structural integrity.

This is also confirmed by XRD and DTA studies. The $Ca(OH)_2$ diffraction line (4.91 Å) is clearly seen between 20 and 200°C, and even at 400°C (Figs 3 and 4). The volume of $Ca(OH)_2$ up to 400°C gradually decreases due to loss of bound water in OH^- form. Instead of a steady $Ca(OH)_2$ solid phase, air voids occur in the concrete. This is accompanied by a contemporary increase in pore median radius and total porosity. The higher the loss in water content bound in $Ca(OH)_2$, the more intense is the pore structure coarsening and the more evident is the loss in compressive strength and the increase in permeability of the specimens. The results of thermal analysis show the same trend towards releasing bound water (Table 4). Total loss of mass values are markedly decreased due to 1.) losses in bound water contents of C–A–H and C–S–H gel – like hydration products between temperature range 100 and 400°C, bearing in mind ettringite and ettringite-related products decomposition over a temperature of 80°C, mainly at interval between 100 and 200°C; 2.) free $Ca(OH)_2$ dehydroxylation over 400 up to 600°C, and 3.) calcite dissociation over 600°C. The X-ray diffraction and thermal analysis results show that the decrease in strength and Young's modulus of elasticity; and contrary the increase in pore median radius and permeability coefficient of concrete depends upon the bound water content values of the ce-

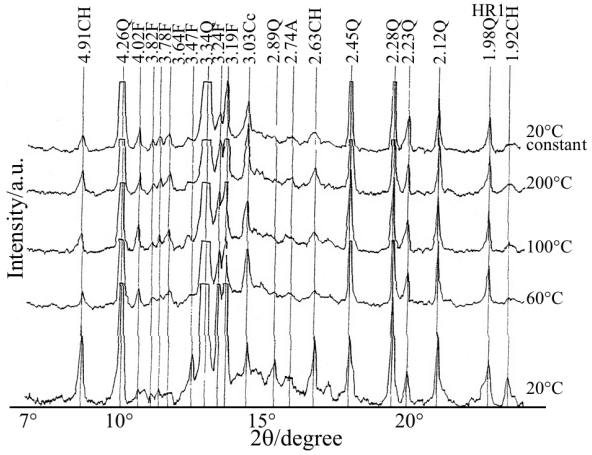

Fig. 3 X -ray diffraction patterns of concrete specimens at heating regime HR 1

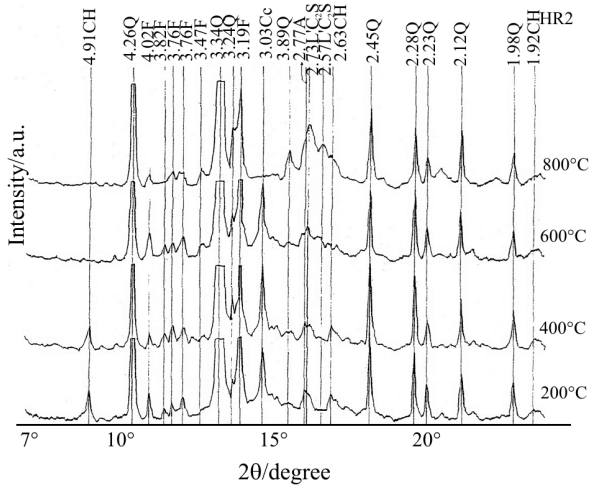

Fig. 4 X-ray diffraction patterns of concrete specimens at heating regime HR 2

Table 4 Results of thermal analysis of tested specimens

Temperature level		Content of bound water in hardened cement paste/ %	Total mass loss/ %	CaO bound in		Total content of CaO in $Ca(OH)_2$ and $CaCO_3$ /%
				$Ca(OH)_2$/%	$CaCO_3$/%	
CONTROL*	= 20°C	3.22	8.14	0.89	1.33	2.22
	40°C	3.40	7.40	0.96	1.12	2.08
HR 1	60°C	3.27	7.59	1.04	1.15	2.19
	100°C	2.93	7.27	0.82	1.01	1.83
	200°C	2.43	6.48	0.72	1.43	2.15
CONST	20°C	3.04	7.68	1.08	1.19	2.27
	200°C	2.73	8.12	1.42	1.45	2.87
	400°C	2.60	9.71	1.37	1.38	2.75
HR 2	600°C	1.27	6.03	1.16	1.12	2.28
	800°C	0.80	1.90	0.37	0.22	0.59

ment paste either in gel-like hydration products (temperature levels between 80 and 400°C) or free $Ca(OH)_2$ (temperature 400–600°C). At temperatures over 600°C, the structural degradation of concrete is markedly influenced by the decomposition of calcite either from carbonation products or calcite/dolomite aggregates, and even at and above 800°C may be also influenced by the re-crystallization of new non-binding phases arising from hydrated cement minerals under re-combustion. Test results reveal that thermal analysis together with measured pore structure variables using MIP is a suitable technique for the evaluation of concrete quality at high-temperature attack.

General discussion

The relations among Young's modulus of elasticity, compressive strength on prisms, pore median radius and bound water content values at 20 and 800°C are depicted in Figs 5 and 6, respectively. Decrease in bound water content (except that of 40°C) connected with the increase in permeability coefficients of the concrete at temperature elevation from 20 to 800°C is given in Fig. 7. By extreme contrast, higher permeability coefficient values are closely connected with pore median radius increase due to high-temperature attack, as seen in Fig. 8. Dependences between decreasing compressive strength and increasing concrete permeability due to temperature elevations are seen in Fig. 9.

The decrease in Young's modulus of elasticity and prism strength depends upon the release of bound water in hydration products of the cement in the temperature range 40–800°C (Fig. 5) and 200–800°C

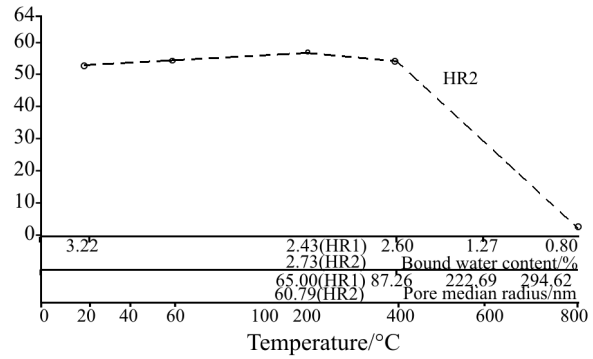

Fig. 6 Relation between compressive strength, bound water content and pore median radius of concrete specimens at temperature up to 800°C

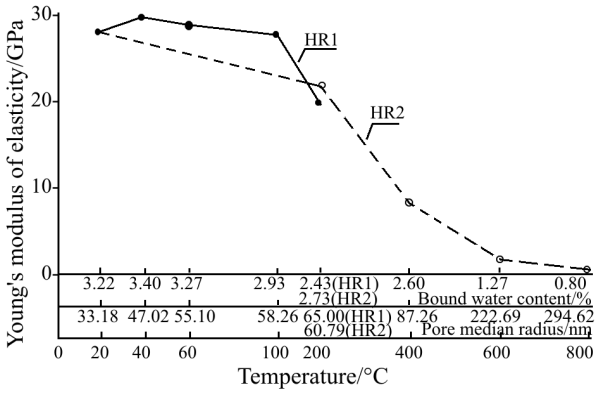

Fig. 5 Relation between Young´s modulus of elasticity, bound water content and pore median radius of concrete specimens between 20 and 800°C

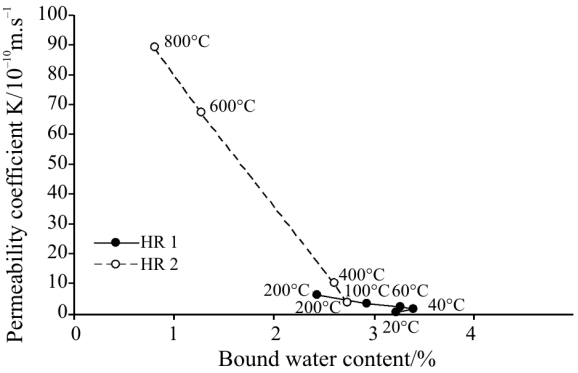

Fig. 7 Relation between permeability coefficient and bound water content of concrete specimens at various temperature levels

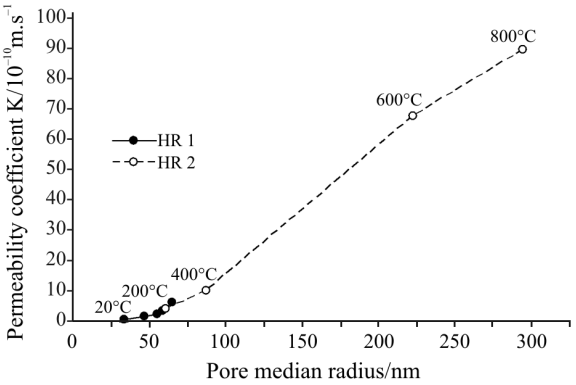

Fig. 8 Relation between permeability coefficient and pore median radius of concrete specimens subjected to temperatures up to 800°C

(Fig. 6), respectively. The temperature-dependent damage of the hydration products integrity is caused by the hydrate phase dewatering with the consequent air voids formation inducing the pore structure coarsening. This is clearly confirmed by pore median radius increases with a rise in temperature. The higher the temperature the more intense dewatering of hydration products and increasing in large pore volume are observed. This effect is evidently observed over the temperature 400°C, mainly between 400 and 600°C when $Ca(OH)_2$ decomposes; and above 600°C when structural damage is influenced by $CaCO_3$ dissociation. At the temperature 200°C, shorter temperature attack at HR2 results in the hydration products richer in bound water content (2.73%) and lower pore median radius (60.79 nm) and total porosity (13.14%) relative to the 28-day thermal treatment of concrete specimens (HR1) characterized by hydration products poorer in bound water content (2.43%) and pore structure with higher pore median radius (65.00 nm) and total porosity (15.23%). Structural degradation of concrete at this temperature is influenced by the duration of temperature attack. Hydrate phase dewatering and pore structure coarsening of the concrete are time-dependent variables. This is clearly confirmed by mutual dependence between bound water content and pore median radius at 200°C**.** Moreover, the higher the temperature, the higher pore median radius and the lower bound water content in concrete specimens are found. Over the temperature 600°C the release of gaseous CO_2 from carbonation products is considered as the reason of the structural integrity damage of the concrete. The content of bound water extremely decreases with a rise in the temperature. This explains a quick reduction in the volume of hydrate phase after a sudden temperature elevation. The lower volume of the hydrate phase and the higher pore median radius are observed, the higher permeability of the concrete specimens is found. Permeability coefficients increase dramatically over the temperature 400°C as seen in Figs 7 and 8. The same results give the comparison of permeability coefficient and strength values (Fig. 9). It is evident that permeability increases and strength decreases mainly over the temperature 400°C when the volume of hydrate phase gradually drops due to loss of chemically bound water in $Ca(OH)_2$. At 600°C when $Ca(OH)_2$ is dehydroxylated the 59.5% loss in compressive strength is found. The concrete strength at 600°C is believed to be the result of residual $Ca(OH)_2$; the compact structure of carbonation products and tobermorite-like phase, and mutual interaction between them. The complete decomposition of $Ca(OH)_2$ and carbonation products dissociation are dominant processes between 600 and 800°C. At 800°C concrete is characterized by the collapse of its structural integrity, revealing residual compressive strength, the value of which is only 19.5% of that at 20°C.

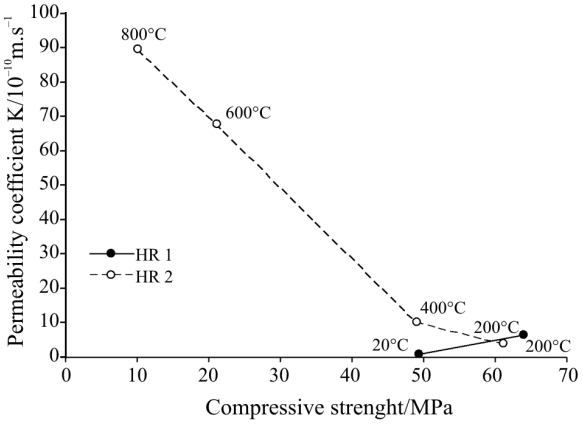

Fig. 9 Relation between permeability coefficient and compressive strength of the concrete at temperature attack between 20 and 800°C

The temperature-dependent damage of the concrete structural integrity depends upon: 1) the loss in the content of water bound in hydration products and $Ca(OH)_2$ and consequent 2) air voids formation due to the substitution of bulky mass of the hydrate phase by large pores and consequent 3) Young's modulus of elasticity and strength decrease due to the pore structure coarsening, and consequent 4) increase in permeability coefficient of the concrete due to the increase in total porosity connected with decrease in strength of the concrete specimens.

The critical temperature when the above changes acquire dramatical character is 400°C. In any case the concrete kept over temperatures 40°C up to 200 and 400°C has sustainably increased permeability that can be regarded as dangerous for moisture and deleterious gases mobility and ingress to the steel reinforcement during healing at the ambient 20°C after high-temperature attack.

Conclusions

Based on this study, the following conclusions can be drawn:

- Test results reveal that thermal analysis (TA) with a close connection with mercury intrusion porosimetry (MIP), calculated permeability coefficient on the basis of the measured pore structure variables using MIP, the estimation of Young's modulus of elasticity and strength values are suitable techniques for the evaluation of the concrete structural integrity when exposed to high-temperature attack. The TA, MIP with permeability calculations, Young's modulus of elasticity and strength are four basic methods for the evaluation of high-temperature attack (fire) on the concrete giving reliable and mutually consistent results.
- The damage of concrete structural quality is given by a three-stage model. (*i*) The damage to 400°C – when gel-like hydration products are decomposed (*ii*) The damage between 400 and 600°C – when $Ca(OH)_2$ is dehydroxylated. Significant decrease in strength and increase in permeability of concrete over 400°C confirms this temperature to be critical for residual concrete properties after high-temperature attack. (*iii*) The physical state of concrete between 600 and 800°C is characterized by the collapse of structural integrity, revealing residual compressive strength. By contrast with it, permeability coefficients are dramatically increased.
- It is concluded that the temperature-dependent concrete damage is influenced by the cement content and its quality, volume of the admixture and the addition, type and quality of the aggregates including its grading, and volume of the super plasticizer that must be fully compatible with the cement employed. To make high-durable concrete with the critical temperature shifted over 400°C, it is essential to have precisely proposed concrete mixture composition and high quality control materials and concrete-making procedure.

Acknowledgements

The UPTUN-project 'Cost-effective, sustainable and innovative upgrading for fire safety in existing tunnels' is being carried out in the framework of the 'Competitive and Sustainable Growth Programme, Project GRD1-2001-40739, Contract G1RD-CT-2002-0766', with a financial contribution of the European Community.

References

1 R. Felicetti and P. G. Gambarova, ACI Mater. J., 95 (1998) 395.
2 Ch.-S. Poon, S. Azhar, M. Anson and Y-L. Wong, Cem. Concr. Res., 31 (2001) 1291.
3 P. Kalifa, G. Chéné and C. Gallé, Cem. Concr. Res., 31 (2001) 1487.
4 V. Vydra, F. Vodák, O. Kapičkovõ and Š. Hošková, Cem. Concr. Res., 31 (2001) 1023.
5 C. Alonso, C. Andrade, M. Castellone and G. A. Khoury 2003 CISM Workshop on Effect of Heat on Concrete, Udine, 9–13 June.
6 G. A. Khoury and C. E. Majorana, 2003, CISM Workshop on Effect of Heat on Concrete, Udine, 9–13 June.
7 M. Ichikawa and M. Kanaya, Cem. Concr. Res., 27 (1997) 1123.
8 C. Xiadong and R. J. Kirkpatrick, Cem. Concr. Res., 25 (1995) 1137.
9 J. Escalante-Garcia and J. H. Sharp, Cem. Concr. Res., 28 (1998) 1259.
10 S. C. Mojumdar, B. Chowdhury, K. G. Varshney and K. Mazanec, J. Therm. Anal. Cal., 78 (2004) 135.
11 M. Drábik, L'. Gáliková, K. G. Varshney and M. A. Quaraishi, J. Therm. Anal. Cal., 76 (2004) 91.
12 J. Escalante-Garcia and J. H. Sharp, Cem. Concr. Res., 28 (1998) 1275.
13 G. Chanvillard and L. D´Aloia, ACI Mater. J., 94 (1997) 520.
14 J. Odler and J. Skalny, J. Applied Chem. Biotechn., 6 (1973) 661.
15 I. Janotka and L'. Bágel', ACI Mater. J., 99 (2002) 196.
16 S. Y. N. Chan, G. F. Peng and M. Anson, ACI Mater. J., 96 (1999) 403.
17 S. K. Handoo, S. Agarwal and J. K. Agarwal, Cem. Concr. Res., 32 (2002) 1009.
18 I. A. Abo-El-Enein, I. Hanafi and E. E. Hekai, Il Cemento, 2 (1998) 121.
19 W.-M. Lin, T. D. Lin and L. J. Couche, – Powers, ACI Mater. J., 93 (1996) 199.
20 M. U. K. Afridi, Y. Ohama, Z. M. Iqbal and K. Demura, Int. J. Cem. Composites and Lightweight Concr., 11 (1989) 235.
21 M. U. K. Afridi, Y. Ohama, Z. M. Iqbal and K. Demura, Cem. Concr. Res., 20 (1990) 163.
22 R. I . Berger and J. D. McGregor, J. Am. Ceram. Soc., 56 (1973) 73.
23 A. Shayan, W. Quick and C. J. Lancucki, Adv. Cem. Res., 5 (1993) 151.
24 A. N. Noumowé, ACI Mater. J., 100 (2003) 326.
25 G. A. Khoury, B. N. Grainer and P. J. E. Sullivan, Mag. Concr. Res., 37 (1985) 131.

DOI: 10.1007/s10973-005-6997-9